

VolleyBots: A Testbed for Multi-Drone Volleyball Game Combining Motion Control and Strategic Play

Zelai Xu¹ Chao Yu¹ Ruize Zhang¹ Huining Yuan² Xiangmin Yi³ Shilong Ji¹ Chuqi Wang¹ Wenhao Tang¹
Yu Wang¹

Abstract

Multi-agent reinforcement learning (MARL) has made significant progress, largely fueled by the development of specialized testbeds that enable systematic evaluation of algorithms in controlled yet challenging scenarios. However, existing testbeds often focus on purely virtual simulations or limited robot morphologies such as robotic arms, quadrupeds, and humanoids, leaving high-mobility platforms with real-world physical constraints like drones underexplored. To bridge this gap, we present *VolleyBots*, a new MARL testbed where multiple drones cooperate and compete in the sport of volleyball under physical dynamics. *VolleyBots* features a turn-based interaction model under volleyball rules, a hierarchical decision-making process that combines motion control and strategic play, and a high-fidelity simulation for seamless sim-to-real transfer. We provide a comprehensive suite of tasks ranging from single-drone drills to multi-drone cooperative and competitive tasks, accompanied by baseline evaluations of representative MARL and game-theoretic algorithms. Results in simulation show that while existing algorithms handle simple tasks effectively, they encounter difficulty in complex tasks that require both low-level control and high-level strategy. We further demonstrate zero-shot deployment of a simulation-learned policy to real-world drones, highlighting *VolleyBots*' potential to propel MARL research involving agile robotic platforms. The project page is at <https://sites.google.com/view/thu-volleybots/home>.

¹Department of Electronic Engineering, Tsinghua University, Beijing, China ²School of Astronautics, Beihang University, Beijing, China ³School of Artificial Intelligence, Beijing University of Posts and Telecommunications, Beijing, China. Correspondence to: Chao Yu <yuchao@tsinghua.edu.cn>, Yu Wang <yuwang@tsinghua.edu.cn>.

Preliminary work. Under review.

1. Introduction

Multi-agent reinforcement learning (MARL) has demonstrated remarkable success across diverse domains, including competitive board games such as Go (Silver et al., 2016), cooperative card games like Hanabi (Bard et al., 2020), real-time strategy challenges such as the StarCraft Multi-Agent Challenge (SMAC) (Samvelyan et al., 2019; Ellis et al., 2024) and Google Research Football (GRF) (Kurach et al., 2020), as well as human-AI cooperative games like Overcooked (Carroll et al., 2019). These testbeds have collectively propelled MARL research forward by showcasing how agents can effectively learn to cooperate, compete, and adapt within complex multi-agent interactions.

Despite the progress in MARL, most established platforms are fully simulated games that do not account for physical-world interactions. To address this gap, several MARL testbeds based on robotic platforms have been developed, such as Multi-Agent MuJoCo(MAMuJoCo) (Peng et al., 2021), Bimanual Dexterous Hands (Bi-DexHands) (Chen et al., 2022), and Multi-agent Quadruped Environment (MQE) (Xiong et al., 2024). Among these, robot sports stand out as a typical task that integrates strategic decision-making under sport-specific rules—such as teamwork and adversarial play—with complex, dynamic motion control constrained by real-world physical factors. Notable examples include robot table tennis (D'Ambrosio et al., 2024), quadrupedal robot football (Ji et al., 2022), and humanoid football (Liu et al., 2022; Haarnoja et al., 2024). However, robot sports often lack open-source simulation environments and real-world support, limiting their effectiveness as research testbeds. Additionally, these platforms mainly focus on robotic arms, quadrupedal, and humanoid, with limited exploration of high-mobility, agile platforms like drones.

In this work, we introduce a novel MARL testbed named *VolleyBots*, where multiple drones engage in the popular sport of volleyball. This testbed addresses gaps in existing robot sports platforms by incorporating: (i) a turn-based interaction model governed by volleyball rules, effectively capturing discrete offensive and defensive phases for MARL studies; (ii) a hierarchical decision-making process that combines low-level motion control with high-level strategic play

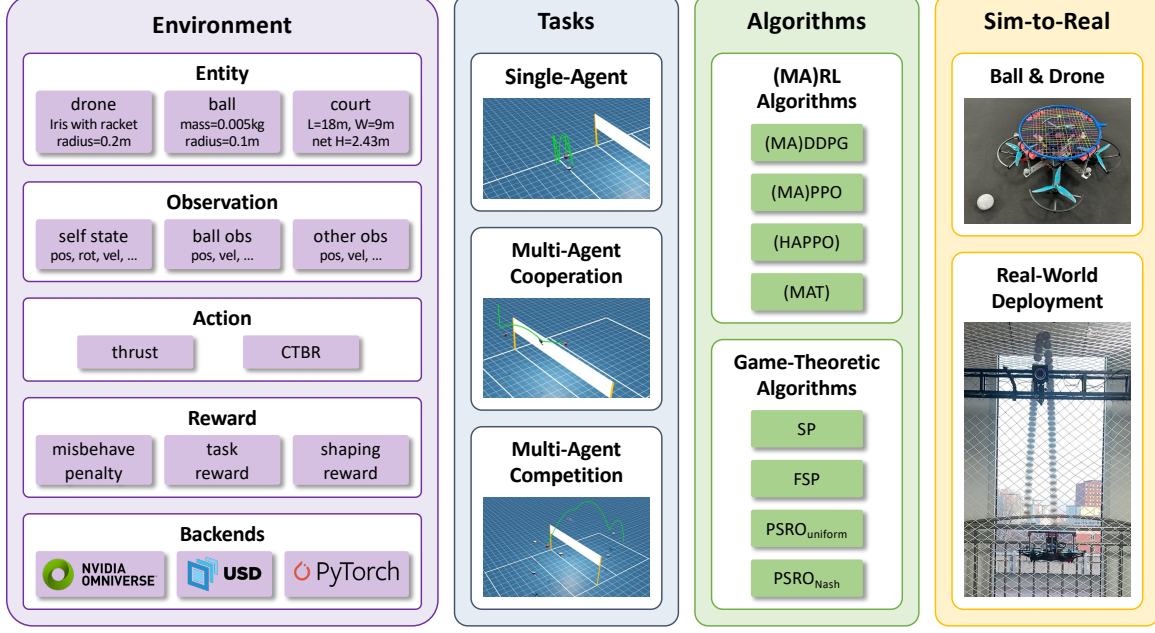


Figure 1. Overview of the VolleyBots Testbed. VolleyBots comprises four key components: (1) Environment, supported by Isaac Sim and PyTorch, which defines entities, observations, actions, and reward functions; (2) Tasks, including 3 single-agent tasks, 3 multi-agent cooperative tasks and 2 multi-agent competitive tasks; (3) Algorithms, encompassing RL, MARL, game-theoretic algorithms; and (4) Sim-to-Real Transfer, enabling zero-shot deployment from simulation to real-world environments.

to execute complex flight maneuvers; and (iii) a high-fidelity simulation that models drone dynamics and interactions between the drones and the ball, and supports flexible parameter randomization, enabling seamless sim-to-real transfer.

The overview of the VolleyBots testbed is shown in Fig. 1. Built on Nvidia Isaac Sim (Mittal et al., 2023), VolleyBots supports GPU-based rapid data collection, making it highly suitable for RL research. Inspired by the way humans progressively learn the rules of volleyball, we designed a series of tasks ranging from single-drone drills to multi-drone cooperative plays and competitive matchups. In addition, we have implemented baseline MARL and game-theoretic algorithms and provided benchmark results for the proposed tasks. The simulation results reveal that existing algorithms perform competently on simple tasks like single-drone control, but struggle to solve complex tasks like multi-drone competitions that require both low-level motion control and high-level strategic play. To demonstrate real-world deployment ability, we show a policy trained to bump volleyball can be deployed on an open-source quadrotor equipped with a racket in a zero-shot manner. We envision VolleyBots as a valuable platform for studying MARL and game-theoretic algorithms with complex drone control tasks.

Our main contributions are summarized as follows:

1. We introduce VolleyBots, a multi-agent drone environment that operates under turn-based interactions,

combines hierarchical decision-making, and is compatible with sim-to-real deployments.

2. We release diverse benchmark tasks and baseline evaluations of representative MARL and game-theoretic algorithms, thereby facilitating reproducible research and comparative assessments.
3. We show the sim-to-real feasibility of transferring learned policies to physical drones, highlighting the environment’s alignment with real-world parameters.

2. Related Work

2.1. Reinforcement Learning for Drone Control Task

Executing precise and agile flight maneuvers is essential for drones, which has driven the development of diverse control strategies (Bouabdallah et al., 2004; Williams et al., 2017; Hwangbo et al., 2017). Among these, RL has shown significant promise, offering flexibility and efficiency in drone control. Drone racing is a notable single-drone control task where RL has achieved human-level performance (Kaufmann et al., 2023), showcasing near-time-optimal decision-making capabilities. Beyond racing, researchers also leveraged RL for executing aggressive flight maneuvers (Sun et al., 2022) and achieving hovering stabilization under highly challenging conditions (Hwangbo et al., 2017). As for multi-drone tasks, RL has been applied to cooperative

	Multi-Agent Task			Action Space	Game Type	Entity	Hierarchical Policy	Open Source
	coop.	comp.	mixed					
Go	✗	✓	✗	discrete	turn-based	simulation	✗	✓
Hanabi	✓	✗	✗	discrete	turn-based	simulation	✗	✓
SMAC	✓	✗	✗	discrete	simultaneous	simulation	✗	✓
Overcooked	✓	✗	✗	discrete	simultaneous	simulation	✗	✓
MPE	✓	✓	✓	discrete	simultaneous	simulation	✗	✓
GRF	✓	✓	✓	discrete	simultaneous	simulation	✗	✓
MAMuJoCo	✓	✗	✗	continuous	simultaneous	ant, walker, etc.	✗	✓
Bi-DexHands	✓	✗	✗	continuous	simultaneous	dexterous hands	✗	✓
Robot Table Tennis	✗	✓	✗	continuous	turn-based	robotic arm	✓	✗
Humanoid Football	✗	✓	✓	continuous	simultaneous	humanoid	✓	✗
SMPOlympics	✗	✓	✓	continuous	simu. & turn-based	humanoid	✗	✓
MQE	✓	✓	✓	continuous	simultaneous	quadruped	✓	✓
VolleyBots (Ours)	✓	✓	✓	continuous	turn-based	drone	✓	✓

Table 1. Comparison of VolleyBots and existing representative MARL testbeds.

tasks such as formation maintenance (Quan et al., 2022), as well as more complex scenarios like multi-drone pursuit-evasion tasks (Chen et al., 2024a), further showcasing its potential to jointly optimize task-level planning and control. In this paper, we present VolleyBots, an MARL testbed designed to study the novel drone control task of drone volleyball. This task introduces unique challenges, requiring drones to learn both cooperative and competitive strategies at the task level while maintaining agile and precise control. Additionally, VolleyBots provides a comprehensive platform with baseline implementations of (MA)RL and game-theoretic algorithms, as well as support for sim-to-real transfer, facilitating the development and evaluation of advanced drone control strategies.

2.2. MARL Testbeds

Many existing MARL testbeds focus on fully simulated environments without real-world physical interactions. For instance, AlphaGo (Silver et al., 2016) explores the turn-based game of Go, sparking deep RL research. Subsequent environments like SMAC (Samvelyan et al., 2019; Ellis et al., 2024), Overcooked (Carroll et al., 2019), and Hanabi (Bard et al., 2020) simulate cooperative scenarios using video games or card games. Multi-agent Particle Environments (MPE) (Lowe et al., 2020) and GRF (Kurach et al., 2020) provide a variety of cooperative, competitive, and mixed cooperative-competitive tasks. These testbeds emphasize high-level decision-making and largely focus on discrete action spaces, overlooking real-world continuous control tasks with physical constraints.

Recently, several MARL environments have been proposed to incorporate real-world physics and interactions. For example, MAMuJoCo (Peng et al., 2021) offers multi-agent continuous control tasks, and Bi-DexHands (Chen et al., 2022) focuses on dexterous bimanual manipulation with

robotic hands. While these testbeds explore continuous action spaces, they are limited to cooperative tasks. Competitive sports, much like their societal role in humans, provide a standard way to evaluate decision-making under dynamic, rule-constrained, and physically realistic conditions. Some works have explored this direction, such as Robot Table Tennis (D’Ambrosio et al., 2024), achieving near human-level performance in ping-pong, and Humanoid Football (Liu et al., 2022; Haarnoja et al., 2024), which models 2 vs 2 football with humanoid robots. Despite bringing MARL closer to real-world applications, these platforms often lack open-source simulations or real-world deployment support. Open-source testbeds like SMPOlympics (Luo et al., 2024) offer physically simulated environments for humanoids to compete in Olympic sports, and MQE (Xiong et al., 2024) proposes multi-agent locomotion tasks with quadrupeds, including 1 vs 1 and 2 vs 2 football competitions. However, existing testbeds primarily focus on robotic arms, quadrupeds, and humanoids, leaving high-mobility, agile robot platforms like drones underexplored.

To address these gaps, we introduce VolleyBots, a turn-based, drone-focused sports environment featuring high-level decision-making and low-level continuous control. A comprehensive comparison between existing MARL testbeds and VolleyBots is shown in Table 1. Built on a realistic physical simulator, VolleyBots supports real-world deployment and offers a complementary testbed for advancing MARL research with agile robotic platforms.

3. VolleyBots Environment

In this section, we introduce the environment design of the VolleyBots testbed. The environment is built upon the high-throughput and GPU-parallelized OmniDrones (Xu et al., 2024) simulator, which relies on Isaac Sim (Mittal et al., 2023) to facilitate rapid data collection. We further config-

ure OmniDrones to simulate realistic flight dynamics and interaction between the drones and the ball, then implement standard volleyball rules and gameplay mechanics to create a challenging domain for drone control tasks. We will describe the simulation entity, observation space, action space, and reward functions in the following subsections.

3.1. Simulation Entity

Our environment simulates real-world physics dynamics and interactions of three key components including the drones, the ball, and the court. We provide a flexible configuration of each entity's model and parameters to enable a wide range of task designs. For the default configuration, we adopt the *Iris* quadrotor model (Furrer et al., 2016) as the primary drone platform, augmented with a virtual “racket” of radius 0.2 m and coefficient of restitution 0.8 for ball striking. The ball is modeled as a sphere with a radius of 0.1 m, a mass of 5 g, and a coefficient of restitution of 0.8, enabling realistic bounces and interactions with both drones and the environment. The court follows standard volleyball dimensions of 9 m \times 18 m with a net height of 2.43 m. All these models and parameters can be easily modified and randomized to facilitate sim-to-real transfer, and a zero-shot real-world deployment example will be presented in Sec. 6.

3.2. Observation Space

To align with the feature of partial observability in real-world volleyball games, we adopt a state-based observation space where each drone can fully observe its own physical state and partially observe the ball's state and other drones' state. More specifically, each drone has full observability of its position, rotation, velocity, angular velocity, and other physical states. For ball observation, each drone can only partially observe the ball's position and velocity. In multi-agent tasks, each drone can also partially observe other drones' position and velocity. Minor variations in the observation space may be required for different tasks, such as the ID of each drone in multi-agent tasks. Detailed observation configurations for each task are provided in the Appendix B.

3.3. Action Space

We provide two types of continuous action spaces that differ in their level of control, with Collective Thrust and Body Rates (CTBR) offering a higher-level abstraction and Per-Rotor Thrust (PRT) offering a more fine-grained manipulation of individual rotors.

Collective Thrust and Body Rates. A typical mode of drone control is to specify a single collective thrust command along with body rates for roll, pitch, and yaw. This higher-level abstraction hides many hardware-specific parameters of the drone, often leading to more stable training.

It also simplifies sim-to-real transfer by reducing the reliance on precise modeling of individual rotor dynamics.

Per-Rotor Thrust. Alternatively, the drone can directly control each rotor's thrust. This fine-grained control allows the policy to fully exploit the drone's agility and maneuverability. However, it typically demands a more accurate model of the drone's hardware and may increase the difficulty of sim-to-real deployment.

3.4. Reward Functions

The reward function for each task consists of three parts, including the misbehave penalty for general motion control, the task reward for task completion, and the shaping reward to accelerate training.

Misbehave Penalty. This term is consistent across all tasks and penalizes undesirable behaviors related to general drone motion control, such as crashes, collisions, and invalid hits. By imposing penalties for misbehavior, the drones are guided to maintain physically plausible trajectories and avoid actions that could lead to control failure.

Task Reward. Each task features a primary objective-based reward that encourages the successful completion of the task. For example, in solo bump tasks, the drone will get a reward of 1 for each successful hit of the ball. Since the task rewards are typically sparse, agents must rely on effective exploration to learn policies that complete the task.

Shaping Reward. Due to the sparse nature of many task rewards, relying solely on the misbehave penalty and the task reward can make it difficult for agents to successfully complete the tasks. To address this challenge, we introduce additional shaping rewards in multi-agent tasks to help steer the learning process. For example, the drone's movement toward the ball is rewarded when a hit is required. By providing additional guidance, the shaping rewards significantly accelerate learning in complex tasks.

We note that while our reward and observation design is effective for algorithm testing and yields sensible results, it is not optimized for real-world deployment scenarios. To encourage further exploration, we provide a flexible user API to enable experiments with improved designs.

4. VolleyBots Tasks

Inspired by the way humans progressively learn to play volleyball, we introduce a series of tasks that systematically assess both low-level motion control and high-level strategic play, as shown in Fig. 2. These tasks are organized into three categories: single-agent, multi-agent cooperative, and multi-agent competitive. Each category aligns with standard volleyball drills or match settings commonly adopted in human training, ranging from basic ball control, through

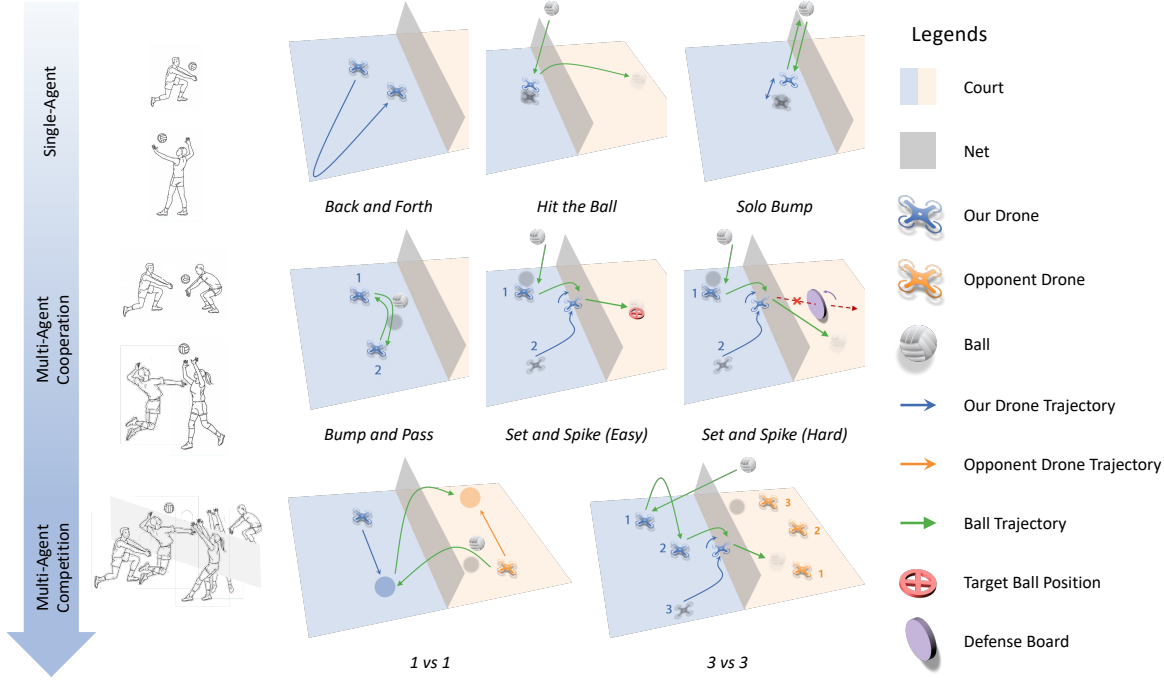


Figure 2. Proposed tasks in the VolleyBots testbed, inspired by the process of human learning in volleyball. Single-agent tasks evaluate low-level control, while multi-agent cooperative and competitive tasks integrate high-level decision-making with low-level control.

cooperative play, to full competitive games. Evaluation metrics vary across tasks to assess performance in motion control, cooperative teamwork, and strategic competition. The detailed configuration and reward design of each task can be found in Appendix B.

4.1. Single-Agent Tasks

Single-agent tasks are designed to follow typical solo training drills used in human volleyball practice, including *Back and Forth*, *Hit the Ball*, and *Solo Bump*. These tasks evaluate the drone’s basic capabilities such as flight stability, motion control, and ball-handling proficiency.

Back and Forth. The drone sprints between two designated points to complete as many round trips as possible within the time limit. This task is analogous to the back-and-forth sprints in volleyball practice and requires basic motion control of the drone. The performance is evaluated by the number of completed round trips within the time limit.

Hit the Ball. The ball is initialized directly above the drone, and the drone hits the ball once to make it land as far as possible. This task is analogous to the typical hitting drill in volleyball and requires both motion control and ball-handling proficiency. The performance is evaluated by the distance of the ball’s landing position from the initial position.

Solo Bump. The ball is initialized directly above the drone, and the drone bumps the ball in place to a specific height

as many times as possible within the time limit. This task is analogous to the solo bump drill in human practice and requires motion control, ball-handling proficiency, and stability. The performance is evaluated by the number of successful bumps within the time limit.

4.2. Multi-Agent Cooperative Tasks

Multi-agent cooperative tasks are inspired by standard two-player training drills used in volleyball teamwork, including *Bump and Pass*, *Set and Spike (Easy)*, and *Set and Spike (Hard)*. Besides basic motion control and ball handling, these tasks also require teamwork and cooperation.

Bump and Pass. Two drones work together to bump and pass the ball to each other back and forth as many times as possible within the time limit. This task is analogous to the two-player bumping practice in volleyball training and requires homogeneous multi-agent cooperation. The performance is evaluated by the number of successful bumps within the time limit.

Set and Spike (Easy). Two drones take on the role of a setter and an attacker. The setter passes the ball to the attacker, and the attacker then spikes the ball downward to the target region on the opposing side. This task is analogous to the setter-attacker offensive drills in volleyball training and requires heterogeneous multi-agent cooperation. The performance is evaluated by the success rate of the downward

	<i>Back and Forth</i>		<i>Hit the Ball</i>		<i>Solo Bump</i>	
	CTBR	PRT	CTBR	PRT	CTBR	PRT
DDPG	0.81 ± 0.06	0.89 ± 0.10	3.48 ± 0.55	2.89 ± 1.07	0.00 ± 0.00	0.02 ± 0.03
PPO	9.10 ± 0.22	9.90 ± 0.05	10.46 ± 0.07	11.43 ± 0.04	11.19 ± 0.31	11.23 ± 0.86

Table 2. Benchmark result of single-agent tasks with different action spaces including Collective Thrust and Body Rates (CTBR) and Per-Rotor Thrust (PRT). *Back and Forth* is evaluated by the number of target points reached, *Hit the Ball* is evaluated by the hitting distance, and *Solo Bump* is evaluated by the number of bumps achieving a certain height.

spike to the target region.

Set and Spike (Hard). Similar to *Set and Spike (Easy)* task, two drones act as a setter and an attacker to set and spike the ball to the opposing side. The difference is that there is a rule-based defense board on the opposing side to intercept the attacker’s spike. The presence of the defense board further improves the difficulty of the task, requiring the drones to optimize their speed, precision, and cooperation to defeat the defense board. The performance is evaluated by the success rate of the downward spike that defeats the defense racket.

4.3. Multi-Agent Competitive Tasks

Multi-agent competitive tasks follow the standard volleyball match rules, including the competitive *1 vs 1* task and the mixed cooperative-competitive *3 vs 3* task. These tasks evaluate both the low-level motion control and the high-level strategic play of the drone policy.

1 vs 1. One drone on each side competes against the other in a volleyball match and wins by hitting the ball in the opponent’s court. When the ball is on its side, the drone is allowed only one hit to return the ball to the opponent’s court. This two-player zero-sum setting creates a purely competitive environment that requires both precise flight control and strategic gameplay. To evaluate the performance of the learned policy, we consider three typical metrics including the exploitability, the average win rate against other learned policies, and the Elo rating (Elo & Sloan, 1978). More specifically, the exploitability is approximated by the gap between the learned best response’s win rate against the evaluated policy and its expected win rate at Nash equilibrium, and the Elo rating is computed by running a round-robin tournament between the evaluated policy and a fixed population of policies.

3 vs 3. Three drones on each side form a team to compete against the other team in a volleyball match. The drones in the same team cooperate to serve, pass, spike, and defend within the standard rule of three hits per side. This is a challenging mixed cooperative-competitive game that requires both cooperation within the same team and competition between the opposing teams. Moreover, the drones are required to excel at both low-level motion control and high-

level game play. We evaluated the policy performance using approximate exploitability, the average win rate against other learned policies, and the Elo rating of the policy.

5. Benchmark Results

We present extensive experiments to benchmark representative (MA)RL and game-theoretic algorithms in our VolleyBots testbed. Specifically, for single-agent tasks, we benchmark two RL algorithms and compare their performance under different action space configurations. For multi-agent cooperative tasks, we evaluate four MARL algorithms and compare their performance with and without reward shaping. For multi-agent competitive tasks, we evaluate four game-theoretic algorithms and provide a comprehensive analysis across multiple evaluation metrics. We identify a key challenge in VolleyBots is the hierarchical decision-making process that requires both low-level motion control and high-level strategic play. We further show the potential of hierarchical policy in our VolleyBots testbed by implementing a simple yet effective baseline for the challenging *3 vs 3* task. Detailed discussion about the benchmark algorithms and more experiment results can be found in Appendix C and D.

5.1. Results of Single-Agent Tasks

We evaluate two RL algorithms including Deterministic Policy Gradient (DDPG) (Lillicrap, 2015) and Proximal Policy Optimization (PPO) (Schulman et al., 2017) in three single-agent tasks. We also compare their performance under different action spaces including CTBR and PRT. The averaged results over three seeds are shown in Table 2.

Using the same number of training frames, the performance of PPO and DDPG shows a clear distinction in all three tasks. PPO consistently achieves high task performance in all tasks, while DDPG struggles to learn effective policies that complete these tasks meaningfully. This disparity can be attributed to PPO’s stable on-policy updates, which facilitate efficient exploration and robust learning, whereas DDPG’s deterministic policy and reliance on off-policy updates result in different learning dynamics.

Comparing different action spaces, the final results indicate

	Bump and Pass		Set and Spike (Easy)		Set and Spike (Hard)	
	w.o. shaping	w. shaping	w.o. shaping	w. shaping	w.o. shaping	w. shaping
MADDPG	0.88 ± 0.07	0.90 ± 0.01	0.23 ± 0.01	0.24 ± 0.01	0.24 ± 0.00	0.23 ± 0.00
MAPPO	11.17 ± 1.03	14.05 ± 0.36	0.25 ± 0.00	0.99 ± 0.00	0.25 ± 0.00	0.75 ± 0.01
HAPPO	6.65 ± 3.59	12.35 ± 0.67	0.25 ± 0.00	0.98 ± 0.00	0.25 ± 0.00	0.82 ± 0.11
MAT	7.68 ± 4.9	13.41 ± 0.14	0.25 ± 0.00	0.99 ± 0.00	0.25 ± 0.00	0.75 ± 0.00

Table 3. Benchmark result of multi-agent cooperative tasks with different reward settings including without and with shaping reward. *Bump and Pass* is evaluated by the number of bumps, *Set the Spike (Easy)* and *Set the Spike (Hard)* are evaluated by the success rate.

	1 vs 1			3 vs 3		
	Exploitability ↓	Win Rate ↑	Elo ↑	Exploitability ↓	Win Rate ↑	Elo ↑
SP	48.63	0.55	1072	25.76	0.59	1077
FSP	30.41	0.63	927	38.86	0.52	906
PSRO _{Uniform}	18.51	0.35	854	49.48	0.28	750
PSRO _{Nash}	10.74	0.47	1147	35.83	0.61	1268

Table 4. Benchmark result of multi-agent competitive tasks including *1 vs 1* and *3 vs 3* with different evaluation metrics.

that PRT slightly outperforms CTBR in most tasks. This outcome is likely due to PRT providing more granular control over each motor’s thrust, enabling the drone to maximize task-specific performance with precise adjustments. On the other hand, CTBR demonstrates a slightly faster learning speed in some tasks, as its higher-level abstraction simplifies the control process and reduces the learning complexity. For optimal task performance, we use PRT as the default action space in subsequent experiments. More experiment results and learning curves are provided in Appendix D.2.

5.2. Results of Multi-Agent Cooperative Tasks

We evaluate four MARL algorithms including Multi-Agent DDPG (MADDPG) (Lowe et al., 2017), Multi-Agent PPO (MAPPO) (Yu et al., 2022), Heterogeneous-Agent PPO (HAPPO) (Kuba et al., 2021), Multi-Agent Transformer (MAT) (Wen et al., 2022) in three multi-agent cooperative tasks. We also compare their performance with and without reward shaping. The averaged results over three seeds are shown in Table 3.

Comparing the MARL algorithms, on-policy methods like MAPPO, HAPPO, and MAT successfully complete all three cooperative tasks and exhibit comparable performance, while off-policy method like MADDPG fails to complete these tasks. These results are consistent with the observation in single-agent experiments, and we use MAPPO as the default algorithm in subsequent experiments for its consistently strong performance and efficiency.

As for different reward functions, it is clear that using reward shaping leads to better performance, especially in more complex tasks like *Set and Spike (Hard)*. This is because the misbehave penalty and task reward alone are usually sparse

and make exploration in continuous space particularly challenging. Such sparse setups can serve as benchmarks to evaluate the exploration ability of MARL algorithms. On the other hand, shaping rewards provide intermediate feedback that guides agents toward task-specific objectives more efficiently, and we use shaping rewards in subsequent experiments for efficient learning. More experimental results and learning curves are provided in Appendix D.3.

5.3. Results of Multi-Agent Competitive Tasks

We evaluate four game-theoretic algorithms including self-play (SP), Fictitious Self-Play (FSP) (Heinrich et al., 2015), Policy-Space Response Oracles (PSRO) (Lanctot et al., 2017) with a uniform meta-solver (PSRO_{Uniform}), and a Nash meta-solver (PSRO_{Nash}) in multi-agent competitive tasks. Their performance is evaluated by approximate exploitability, the average win rate against other learned policies, and Elo rating. The results are shown in Table 4. More results and implementation details are provided in Appendix D.4.

In the *1 vs 1* task, all algorithms manage to learn basic behaviors like returning the ball and positioning for subsequent volleys. However, the exploitability metrics indicate that the learned policies are still far from achieving a Nash equilibrium, suggesting that the strategies lack robustness in this two-player zero-sum game. This performance gap highlights the inherent challenge of hierarchical decision-making in this task, where drones must simultaneously execute precise low-level motion control and engage in high-level strategic gameplay under volleyball rules. This challenge presents new opportunities for designing algorithms that can better integrate hierarchical decision-making capabilities.

In the *3 vs 3* task, algorithms exhibit minimal progress,

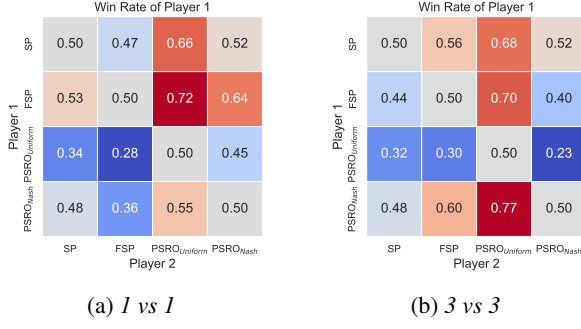


Figure 3. Cross-play heatmap of multi-agent competitive tasks.

such as learning to serve the ball, but fail to produce other strategic behaviors. This outcome underscores the compounded challenges in this scenario, where each team of three drones must not only cooperate internally but also compete against the opposing team. The increased difficulty of achieving high-level strategic play in such a mixed cooperative-competitive environment further amplifies the hierarchical challenges observed in *1 vs 1*. As a result, the *3 vs 3* task serves as a highly demanding benchmark that highlights the need for new approaches for learning in complex multi-agent settings with a hierarchical decision process.

5.4. Hierarchical Policy

We further investigate hierarchical policies as a promising approach. Using the *3 vs 3* task as an example, we first employ the PPO algorithm to develop a set of low-level skill policies, including *Hover*, *Serve*, *Pass*, *Set*, and *Attack*. The details of low-level skills can be found in Appendix D.5. Next, we design a rule-based high-level strategic policy to assign low-level skills to each drone. For the *Serve* and *Attack* skills, the high-level policy also determines whether to hit the ball to the left or right, with an equal probability of 0.5 for each direction. Fig. 4 illustrates two typical demonstrations of the hierarchical policy attaching the *Serve* skill to drone 1 in a serve scenario and the *Attack* skill to drone 3 in a rally scenario. In accordance with volleyball rules, the high-level policy uses an event-driven mechanism, triggering decisions whenever the ball is hit. We evaluate the average win rate of 1000 episodes where the hierarchical policy competes against the SP policy. The results show that the hierarchical policy achieves a significantly higher win rate of 86%. While the current design of the hierarchical policy is in its early stages, it demonstrates substantial potential and offers valuable inspiration for future developments.

6. Sim-to-Real

We use the *Solo Bump* task as a demonstration of the policy’s ability to zero-shot transfer to the real world. We use a quadrotor with a rigidly mounted badminton racket, as

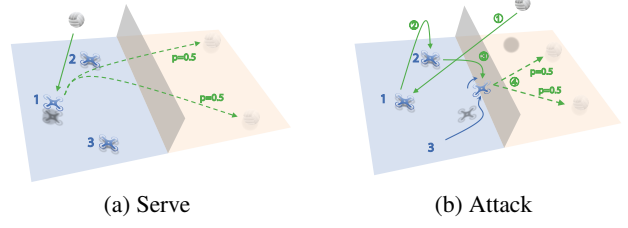


Figure 4. Demonstration of the hierarchical policy selecting *Serve* and *Attack* skills in the *3 vs 3* task.

shown in Fig. 1. The state of both the drone and the ball is captured using a motion capture system. The drone is modeled as a rigid body, with its position and orientation provided by the motion capture system. The drone’s velocity is estimated using an Extended Kalman Filter (EKF) that fuses pose data from the motion capture system and IMU data from the PX4 Autopilot. The ball is modeled as a point mass, with its position sent by the motion capture system and its velocity indirectly computed through a Kalman Filter. The drone’s dynamics parameters and the ball’s properties are determined through system identification.

To simulate real-world noise and imperfect execution of actions, small randomizations are introduced in the ball’s initial position, coefficient of restitution, and the ball’s rebound velocity after each collision with the drone. Inspired by (Chen et al., 2024b), we also add a smoothness reward to encourage smooth actions. The policy uses CTBR as output and is deployed on the onboard Nvidia Orin processor. Experiment results show that the drone successfully performs bump tasks multiple times, providing initial evidence of sim-to-real transfer capability. To support further research, we make the drone configuration, model checkpoint, and real-world deployment videos publicly available on our website. We hope this will accelerate progress in this field.

7. Conclusion

We introduce VolleyBots, a new MARL testbed where drones cooperate and compete in volleyball under real-world physical dynamics. VolleyBots bridges the gap between existing MARL testbeds by introducing a turn-based interaction model, a hierarchical decision-making process, and a high-fidelity simulation for seamless sim-to-real transfer. Through extensive benchmarks from single-agent tasks to multi-agent cooperative and competitive tasks, we show that existing algorithms struggle to solve complex tasks that require both low-level motion control and high-level strategic play. We also showcase the feasibility of deploying policies trained in simulations directly onto physical drones, emphasizing VolleyBots’ sim-to-real transfer and practical utility in real-world applications. We envision VolleyBots as a realistic and challenging testbed for MARL research in high-mobility, agile robotic platforms like drones.

Acknowledgment

We sincerely thank Feng Gao, Yuqing Xie, Yinuo Chen, and Sirui Xiang for their valuable discussions, as well as their assistance in experiments and real-world deployment, which have greatly contributed to the development of this work. Their support and collaboration have been instrumental in refining our ideas and improving the quality of this paper.

This research was supported by National Natural Science Foundation of China (No.62406159, 62325405), Postdoctoral Fellowship Program of CPSF under Grant Number (GZC20240830, 2024M761676), China Postdoctoral Science Special Foundation 2024T170496.

Impact Statement

This work introduces VolleyBots, an MARL testbed specifically designed to push the boundaries of multi-agent reinforcement learning involving high-mobility robotic platforms such as drones. The broader impacts of this research include advancing the intersection of MARL and robotics, enhancing the decision-making capabilities of drones in complex scenarios. By bridging MARL with real-world robotic challenges, this work aims to inspire future breakthroughs in both robotics and multi-agent AI systems.

References

Bard, N., Foerster, J. N., Chandar, S., Burch, N., Lanctot, M., Song, H. F., Parisotto, E., Dumoulin, V., Moitra, S., Hughes, E., et al. The hanabi challenge: A new frontier for ai research. *Artificial Intelligence*, 280:103216, 2020.

Bouabdallah, S., Murrieri, P., and Siegwart, R. Design and control of an indoor micro quadrotor. In *IEEE International Conference on Robotics and Automation, 2004. Proceedings. ICRA'04. 2004*, volume 5, pp. 4393–4398. IEEE, 2004.

Carroll, M., Shah, R., Ho, M. K., Griffiths, T., Seshia, S., Abbeel, P., and Dragan, A. On the utility of learning about humans for human-ai coordination. *Advances in neural information processing systems*, 32, 2019.

Chen, J., Yu, C., Li, G., Tang, W., Yang, X., Xu, B., Yang, H., and Wang, Y. Multi-uav pursuit-evasion with online planning in unknown environments by deep reinforcement learning, 2024a. URL <https://arxiv.org/abs/2409.15866>.

Chen, J., Yu, C., Xie, Y., Gao, F., Chen, Y., Yu, S., Tang, W., Ji, S., Mu, M., Wu, Y., Yang, H., and Wang, Y. What matters in learning a zero-shot sim-to-real rl policy for quadrotor control? a comprehensive study, 2024b. URL <https://arxiv.org/abs/2412.11764>.

Chen, Y., Wu, T., Wang, S., Feng, X., Jiang, J., McAleer, S. M., Geng, Y., Dong, H., Lu, Z., Zhu, S.-C., and Yang, Y. Towards human-level bimanual dexterous manipulation with reinforcement learning, 2022. URL <https://arxiv.org/abs/2206.08686>.

Czarnecki, W. M., Gidel, G., Tracey, B., Tuyls, K., Omidshafiei, S., Balduzzi, D., and Jaderberg, M. Real world games look like spinning tops. *Advances in Neural Information Processing Systems*, 33:17443–17454, 2020.

D'Ambrosio, D. B., Abeyruwan, S., Graesser, L., Iscen, A., Amor, H. B., Bewley, A., Reed, B. J., Reymann, K., Takayama, L., Tassa, Y., et al. Achieving human level competitive robot table tennis. *arXiv preprint arXiv:2408.03906*, 2024.

Ellis, B., Cook, J., Moalla, S., Samvelyan, M., Sun, M., Mahajan, A., Foerster, J., and Whiteson, S. Smacv2: An improved benchmark for cooperative multi-agent reinforcement learning. *Advances in Neural Information Processing Systems*, 36, 2024.

Elo, A. E. and Sloan, S. The rating of chessplayers: Past and present. 1978.

Furrer, F., Burri, M., Achtelik, M., and Siegwart, R. Rotors—a modular gazebo mav simulator framework. *Robot Operating System (ROS) The Complete Reference (Volume 1)*, pp. 595–625, 2016.

Haarnoja, T., Moran, B., Lever, G., Huang, S. H., Tirumala, D., Humplik, J., Wulfmeier, M., Tunyasuvunakool, S., Siegel, N. Y., Hafner, R., et al. Learning agile soccer skills for a bipedal robot with deep reinforcement learning. *Science Robotics*, 9(89):eadi8022, 2024.

Heinrich, J., Lanctot, M., and Silver, D. Fictitious self-play in extensive-form games. In *International conference on machine learning*, pp. 805–813. PMLR, 2015.

Hwangbo, J., Sa, I., Siegwart, R., and Hutter, M. Control of a quadrotor with reinforcement learning. *IEEE Robotics and Automation Letters*, 2(4):2096–2103, 2017.

Ji, Y., Li, Z., Sun, Y., Peng, X. B., Levine, S., Berseth, G., and Sreenath, K. Hierarchical reinforcement learning for precise soccer shooting skills using a quadrupedal robot, 2022. URL <https://arxiv.org/abs/2208.01160>.

Kaufmann, E., Bauersfeld, L., Loquercio, A., Müller, M., Koltun, V., and Scaramuzza, D. Champion-level drone racing using deep reinforcement learning. *Nature*, 620 (7976):982–987, 2023.

Kuba, J. G., Chen, R., Wen, M., Wen, Y., Sun, F., Wang, J., and Yang, Y. Trust region policy optimisation

in multi-agent reinforcement learning. *arXiv preprint arXiv:2109.11251*, 2021.

Kurach, K., Raichuk, A., Stańczyk, P., Zajac, M., Bachem, O., Espeholt, L., Riquelme, C., Vincent, D., Michalski, M., Bousquet, O., et al. Google research football: A novel reinforcement learning environment. In *Proceedings of the AAAI conference on artificial intelligence*, volume 34, pp. 4501–4510, 2020.

Lanctot, M., Zambaldi, V., Gruslys, A., Lazaridou, A., Tuyls, K., Pérolat, J., Silver, D., and Graepel, T. A unified game-theoretic approach to multiagent reinforcement learning. *Advances in neural information processing systems*, 30, 2017.

Lillicrap, T. Continuous control with deep reinforcement learning. *arXiv preprint arXiv:1509.02971*, 2015.

Liu, S., Lever, G., Wang, Z., Merel, J., Eslami, S. A., Hennes, D., Czarnecki, W. M., Tassa, Y., Omidshafiei, S., Abdolmaleki, A., et al. From motor control to team play in simulated humanoid football. *Science Robotics*, 7(69):eab0235, 2022.

Lowe, R., Wu, Y. I., Tamar, A., Harb, J., Pieter Abbeel, O., and Mordatch, I. Multi-agent actor-critic for mixed cooperative-competitive environments. *Advances in neural information processing systems*, 30, 2017.

Lowe, R., Wu, Y., Tamar, A., Harb, J., Abbeel, P., and Mordatch, I. Multi-agent actor-critic for mixed cooperative-competitive environments, 2020. URL <https://arxiv.org/abs/1706.02275>.

Luo, Z., Wang, J., Liu, K., Zhang, H., Tessler, C., Wang, J., Yuan, Y., Cao, J., Lin, Z., Wang, F., Hodgins, J., and Kitani, K. Smplolympics: Sports environments for physically simulated humanoids, 2024. URL <https://arxiv.org/abs/2407.00187>.

McAleer, S., Farina, G., Zhou, G., Wang, M., Yang, Y., and Sandholm, T. Team-psro for learning approximate tmecon in large team games via cooperative reinforcement learning. *Advances in Neural Information Processing Systems*, 36:45402–45418, 2023.

Mittal, M., Yu, C., Yu, Q., Liu, J., Rudin, N., Hoeller, D., Yuan, J. L., Singh, R., Guo, Y., Mazhar, H., Mandlekar, A., Babich, B., State, G., Hutter, M., and Garg, A. Orbit: A unified simulation framework for interactive robot learning environments. *IEEE Robotics and Automation Letters*, 8(6):3740–3747, June 2023. ISSN 2377-3774. doi: 10.1109/LRA.2023.3270034. URL <http://dx.doi.org/10.1109/LRA.2023.3270034>.

Peng, B., Rashid, T., Schroeder de Witt, C., Kamienny, P.-A., Torr, P., Böhmer, W., and Whiteson, S. Facmac: Factored multi-agent centralised policy gradients. *Advances in Neural Information Processing Systems*, 34: 12208–12221, 2021.

Quan, L., Yin, L., Xu, C., and Gao, F. Distributed swarm trajectory optimization for formation flight in dense environments. In *2022 International Conference on Robotics and Automation (ICRA)*, pp. 4979–4985. IEEE, 2022.

Samvelyan, M., Rashid, T., De Witt, C. S., Farquhar, G., Nardelli, N., Rudner, T. G., Hung, C.-M., Torr, P. H., Foerster, J., and Whiteson, S. The starcraft multi-agent challenge. *arXiv preprint arXiv:1902.04043*, 2019.

Schulman, J., Wolski, F., Dhariwal, P., Radford, A., and Klimov, O. Proximal policy optimization algorithms. *arXiv preprint arXiv:1707.06347*, 2017.

Sheehan, H. Elopy: A python library for elo rating systems. <https://github.com/HankSheehan/EloPy>, 2017. Accessed: 2025-01-28.

Silver, D., Huang, A., Maddison, C. J., Guez, A., Sifre, L., Van Den Driessche, G., Schrittwieser, J., Antonoglou, I., Panneershelvam, V., Lanctot, M., et al. Mastering the game of go with deep neural networks and tree search. *nature*, 529(7587):484–489, 2016.

Sun, Q., Fang, J., Zheng, W. X., and Tang, Y. Aggressive quadrotor flight using curiosity-driven reinforcement learning. *IEEE Transactions on Industrial Electronics*, 69(12):13838–13848, 2022.

Wen, M., Kuba, J., Lin, R., Zhang, W., Wen, Y., Wang, J., and Yang, Y. Multi-agent reinforcement learning is a sequence modeling problem. *Advances in Neural Information Processing Systems*, 35:16509–16521, 2022.

Williams, G., Wagener, N., Goldfain, B., Drews, P., Rehg, J. M., Boots, B., and Theodorou, E. A. Information theoretic mpc for model-based reinforcement learning. In *2017 IEEE International Conference on Robotics and Automation (ICRA)*, pp. 1714–1721, 2017. doi: 10.1109/ICRA.2017.7989202.

Xiong, Z., Chen, B., Huang, S., Tu, W.-W., He, Z., and Gao, Y. Mqe: Unleashing the power of interaction with multi-agent quadruped environment. *arXiv preprint arXiv:2403.16015*, 2024.

Xu, B., Gao, F., Yu, C., Zhang, R., Wu, Y., and Wang, Y. Omnidrones: An efficient and flexible platform for reinforcement learning in drone control. *IEEE Robotics and Automation Letters*, 2024.

Xu, Z., Liang, Y., Yu, C., Wang, Y., and Wu, Y. Fictitious cross-play: Learning global nash equilibrium in mixed cooperative-competitive games. *arXiv preprint arXiv:2310.03354*, 2023.

Yu, C., Velu, A., Vinitsky, E., Gao, J., Wang, Y., Bayen, A., and Wu, Y. The surprising effectiveness of ppo in cooperative multi-agent games. *Advances in Neural Information Processing Systems*, 35:24611–24624, 2022.

Zhang, R., Xu, Z., Ma, C., Yu, C., Tu, W.-W., Huang, S., Ye, D., Ding, W., Yang, Y., and Wang, Y. A survey on self-play methods in reinforcement learning. *arXiv preprint arXiv:2408.01072*, 2024.

A. Details of VolleyBots Environment

A.1. Court

The volleyball court in our environment is depicted in Fig. 5. The court is divided into two equal halves by the y -axis, which serves as the dividing line separating the two teams. The coordinate origin is located at the midpoint of the dividing line, and the x -axis extends along the length of the court. The total court length is 18 m, with $x = -9$ and $x = 9$ marking the ends of the court. The y -axis extends across the width of the court, with a total width of 9 m, spanning from $y = -4.5$ to $y = 4.5$. The net is positioned at the center of the court along the y -axis, with a height of 2.43 m, and spans horizontally from $(0, -4.5)$ to $(0, 4.5)$.

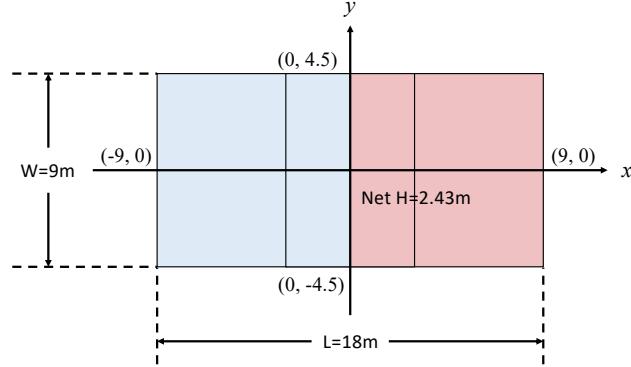


Figure 5. Volleyball court layout in our environment with coordinates.

A.2. Drone

We use the *Iris* quadrotor model (Furrer et al., 2016) as the primary drone platform, augmented with a virtual “racket” of radius 0.2 m and coefficient of restitution 0.8 for ball striking. The drone’s root state is a vector with dimension 23, including its position, rotation, linear velocity, angular velocity, forward orientation, upward orientation, and normalized rotor speeds.

The control dynamics of a multi-rotor drone are governed by its physical configuration and the interaction of various forces and torques. The system’s dynamics can be described as follows:

$$\dot{\mathbf{x}}_W = \mathbf{v}_W, \quad \dot{\mathbf{v}}_W = \mathbf{R}_{WB}\mathbf{f} + \mathbf{g} + \mathbf{F} \quad (1)$$

$$\dot{\mathbf{q}} = \frac{1}{2}\mathbf{q} \otimes \boldsymbol{\omega}, \quad \dot{\boldsymbol{\omega}} = \mathbf{J}^{-1}(\boldsymbol{\eta} - \boldsymbol{\omega} \times \mathbf{J}\boldsymbol{\omega}) \quad (2)$$

where \mathbf{x}_W and \mathbf{v}_W represent the position and velocity of the drone in the world frame, \mathbf{R}_{WB} is the rotation matrix converting from the body frame to the world frame, \mathbf{J} is the diagonal inertia matrix, \mathbf{g} denotes gravity, \mathbf{q} is the orientation represented by quaternions, and $\boldsymbol{\omega}$ is the angular velocity. The quaternion multiplication operator is denoted by \otimes . External forces \mathbf{F} , including aerodynamic drag and downwash effects, are also considered. The collective thrust \mathbf{f} and body rate $\boldsymbol{\eta}$ are computed based on per-rotor thrusts \mathbf{f}_i as:

$$\mathbf{f} = \sum_i \mathbf{R}_B^{(i)} \mathbf{f}_i \quad (3)$$

$$\boldsymbol{\eta} = \sum_i \mathbf{T}_B^{(i)} \times \mathbf{f}_i + k_i \mathbf{f}_i \quad (4)$$

where $\mathbf{R}_B^{(i)}$ and $\mathbf{T}_B^{(i)}$ are the local orientation and translation of the i -th rotor in the body frame, and k_i is the force-to-moment ratio.

Type	Name	Sparse	Value Range	Description
Misbehave Penalty	drone_misbehave	✓	{0, -10}	drone too low or drone too remote
Task Reward	dist_to_target target_stay	✗ ✓	[0, 0.5] × # step {0, 2.5} × # in_target	∞ drone's distance to the current target drone stays in the current target region

 Table 5. Reward of single-agent *Back and Forth* task.

Type	Name	Sparse	Value Range	Description
Misbehave Penalty	ball_misbehave drone_misbehave wrong_hit	✓ ✓ ✓	{0, -10} {0, -10} {0, -10}	ball too low or touch the net or out of court drone too low or touches the net drone does not use the racket to hit the ball
Task Reward	success_hit distance dist_to_anchor	✓ ✓ ✗	{0, 1} [0, +∞] [−∞, 0]	drone hits the ball ∞ the landing position's distance to the anchor ∞ drone's distance to the anchor

 Table 6. Reward of single-agent *Hit the Ball* task.

A.3. Defense Racket

We assume a thin cylindrical racket to mimic a human-held racket for adversarial interactions with a drone. When the ball is hit toward the racket's half of the court, the racket is designed to intercept the ball at a predefined height h_{pre} . Since the ball's position and velocity data can be directly acquired, the descent time t_{pre} , landing point \mathbf{p}_{ball_land} , and pre-collision velocity \mathbf{v}_{ball_pre} can be calculated using projectile motion equations. Additionally, to ensure the ball is returned to a designated position \mathbf{p}_{bdes} and crosses the net, the post-collision motion duration t_{post} of the ball is set to a sufficiently large value. This allows the projectile motion equations to similarly determine the post-collision velocity \mathbf{v}_{ball_post} . Based on these conditions, the required collision position $\mathbf{p}_{collision}$, orientation $\theta_{collision}$ and velocity $\mathbf{v}_{collision}$ of the racket can be derived as follows:

$$\mathbf{p}_{collision} = \mathbf{p}_{ball_land} \quad (5)$$

$$\mathbf{n}_{collision} = \frac{\mathbf{v}_{ball_post} - \mathbf{v}_{ball_pre}}{\|\mathbf{v}_{ball_post} - \mathbf{v}_{ball_pre}\|} = [\sin p \cos r, -\sin r, \cos p \cos r] \quad (6)$$

$$\theta_{collision} = [-\arcsin \mathbf{n}_{collision}(2), \arctan \frac{\mathbf{n}_{collision}(1)}{\mathbf{n}_{collision}(3)}, 0] \quad (7)$$

$$\mathbf{v}_{collision} = \frac{1}{1 + \beta} (\beta \mathbf{v}_{ball_pre} + \mathbf{v}_{ball_post}) \quad (8)$$

where $\mathbf{n}_{collision}$ represents the normal vector of the racket during impact, r denotes the roll angle of the racket, p denotes the pitch angle, while the yaw angle remains fixed at 0, and β represents the restitution coefficient. To simulate the adversarial interaction as realistically as possible, we impose direct constraints on the racket's linear velocity and angular velocity. Based on the simulation time step t_{step} and the descent time t_{post} of the ball, we can calculate the required displacement $\mathbf{d} = \frac{\mathbf{p}_{bdes} - \mathbf{p}_{ball_land}}{t_{post}} t_{step}$ and rotation angle $\theta = \frac{\theta_{collision}}{t_{post}} t_{step}$ that the racket must achieve within each time step. If both \mathbf{d} and θ do not exceed their respective limits (\mathbf{d}_{max} and θ_{max}), the racket moves with linear velocity \mathbf{d} and angular velocity θ . Otherwise, the values are set to their corresponding limits \mathbf{d}_{max} and θ_{max} .

B. Details of Task Design

B.1. Back and Forth

Task Definition. The drone is initialized at an anchor position (4.5, 0, 2), i.e., the center of the red court with a height of 2 m. The other anchor position is (9.0, 4.5, 2), with the target points switching between two designated anchor positions.

Type	Name	Sparse	Value Range	Description
Misbehave Penalty	ball_misbehave	✓	{0, -10}	ball too low or touch the net or out of court
	drone_misbehave	✓	{0, -10}	drone too low or touches the net
	wrong_hit	✓	{0, -10}	drone does not use the racket to hit the ball
Task Reward	success_hit	✓	{0, 1} × # hit	drone hits the ball
	success_height	✓	{0, 1} × # hit	ball reaches the minimum height
	dist_to_anchor	✗	[-∞, 0]	∞ drone's distance to the anchor

 Table 7. Reward of single-agent *Solo Bump* task.

Type	Name	Sparse	Shared	Value Range	Description
Misbehave Penalty	ball_misbehave	✓	✓	{0, -10}	ball too low or touches the net or out of court
	drone_misbehave	✓	✗	{0, -10}	drone too low or touches the net
	wrong_hit	✓	✗	{0, -10}	drone hits in the wrong turn
Task Reward	success_hit	✓	✓	{0, 1} × # hit	drone hits the ball
	success_cross	✓	✓	{0, 1} × # hit	ball crosses the height
	dist_to_anchor	✗	✓	[-∞, 0]	∞ drone's distance to its anchor
Shaping Reward	hit_direction	✓	✗	{0, 1} × # hit	drone hits the ball towards the other drone
	dist_to_ball	✗	✗	[0, 0.05] × # step	∞ drone's distance to the ball

 Table 8. Reward of multi-agent *Bump and Pass* task.

The drone is required to sprint between two designated anchors to complete as many round trips as possible. 5 steps within a sphere with a 0.6 m radius near the anchor position are required for each stay. The maximum episode length is 800 steps.

Observation and Reward. When the action space is Per-Rotor Thrust(PRT), the observation is a vector of dimension 26, which includes the drone's root state and its relative position to the target anchor. When the action space is Collective Thrust and Body Rates (CTBR), the observation dimension is reduced to 22, excluding the drone's throttle. The detailed description of the reward function of this task is listed in Table 5.

Evaluation Metric. This task is evaluated by the number of target points reached within the time limit. A successful stay is defined as the drone staying 5 steps within a sphere with a 0.6 m radius near the target anchor.

B.2. Hit the Ball

Task Definition. The drone is initialized randomly around an anchor position (4.5, 0, 2), i.e., the center of the red court with a height of 2 m. The drone's initial position is sampled uniformly random from [4, -0.5, 1.8] to [5, 0.5, 2.2]. The ball is initialized at (4.5, 0, 5), i.e., 3 m above the anchor position. The ball starts with zero velocity and falls freely. The drone is required to perform a single hit to strike the ball toward the opponent's court, i.e., in the negative direction of the x-axis, aiming for maximum distance. The maximum episode length is 800 steps.

Observation and Reward. When the action space is Per-Rotor Thrust(PRT), the observation is a vector of dimension 32, which includes the drone's root state, the drone's relative position to the anchor, the ball's relative position to the drone, and the ball's velocity. When the action space is Collective Thrust and Body Rates (CTBR), the observation dimension is reduced to 28, excluding the drone's throttle. The detailed description of the reward function of this task is listed in Table 6.

Evaluation Metric. This task is evaluated by the distance between the ball's landing position and the anchor position. The ball's landing position is defined as the intersection of its trajectory with the plane $z = 2$.

Type	Name	Sparse	Shared	Value Range	Description
Misbehave Penalty	ball_misbehave	✓	✓	$\{0, -10\}$	ball too low or touches the net or out of court
	drone_misbehave	✓	✗	$\{0, -10\}$	drone too low or touches the net
	wrong_hit	✓	✗	$\{0, -10\}$	drone hits in the wrong turn
Task Reward	success_hit	✓	✓	$\{0, 5\} \times \# \text{ hit}$	drone hits the ball
	downward_spike	✓	✓	$\{0, 5\} \times \# \text{ spike}$	ball's velocity is downward after spike
	success_cross	✓	✓	$\{0, 5\}$	ball crosses the net
	in_target	✓	✓	$\{0, 5\}$	ball lands in the target region
Shaping Reward	dist_to_anchor	✗	✓	$[-\infty, 0]$	\propto drone's distance its anchor
	hit_direction	✓	✗	$\{0, 1\} \times \# \text{ hit}$	drone hits the ball towards its target
	spike_velociy	✓	✓	$[0, +\infty] \times \# \text{ spike}$	\propto ball's downward velocity after spike
	dist_to_ball	✗	✗	$[0, 0.05] \times \# \text{ step}$	\propto drone's distance to the ball
	dist_to_target	✗	✓	$[0, 2]$	\propto ball's landing position to the target

 Table 9. Reward of multi-agent *Set and Spike (Easy)* task.

Type	Name	Sparse	Shared	Value Range	Description
Misbehave Penalty	ball_misbehave	✓	✓	$\{0, -10\}$	ball too low or touches the net or out of court
	drone_misbehave	✓	✗	$\{0, -10\}$	drone too low or touches the net
	wrong_hit	✓	✗	$\{0, -10\}$	drone hits in the wrong turn
Task Reward	success_hit	✓	✓	$\{0, 5\} \times \# \text{ hit}$	drone hits the ball
	downward_spike	✓	✓	$\{0, 5\} \times \# \text{ spike}$	ball's velocity is downward after spike
	success_cross	✓	✓	$\{0, 5\}$	ball crosses the net
	success_spike	✓	✓	$\{0, 5\}$	defense racket fails to intercept
Shaping Reward	dist_to_anchor	✗	✓	$[-\infty, 0]$	\propto drone's distance to its anchor
	hit_direction	✓	✗	$\{0, 1\} \times \# \text{ hit}$	drone hits the ball towards their targets
	spike_velociy	✓	✓	$[0, +\infty] \times \# \text{ spike}$	\propto ball's downward velocity after spike
	dist_to_ball	✗	✗	$[0, 0.05] \times \# \text{ step}$	\propto drone's distance to the ball

 Table 10. Reward of multi-agent *Set and Spike (Hard)* task.

B.3. Solo Bump

Task Definition. The drone is initialized randomly around an anchor position $(4.5, 0, 2)$, i.e., the center of the red court with a height of 2 m . The drone's initial position is sampled uniformly random from $[4, -0.5, 1.8]$ to $[5, 0.5, 2.2]$. The ball is initialized at $(4.5, 0, 4)$, i.e., 2 m above the anchor position. The ball starts with zero velocity and falls freely. The drone is required to stay within a sphere with 1 m radius near the anchor position and bump the ball as many times as possible. A minimum height of 4 m is required for each bump. The maximum episode length is 800 steps.

Observation and Reward. When the action space is Per-Rotor Thrust (PRT), the observation is a vector of dimension 32, which includes the drone's root state, the drone's relative position to the anchor, the ball's relative position to the drone, and the ball's velocity. When the action space is Collective Thrust and Body Rates (CTBR), the observation dimension is reduced to 28, excluding the drone's throttle. The detailed description of the reward function of this task is listed in Table 7.

Evaluation Metric. This task is evaluated by the number of successful consecutive bumps performed by the drone. A successful bump is defined as the drone hitting the ball such that the ball's highest height exceeds 4 m .

Type	Name	Sparse	Shared	Value Range	Description
Misbehave	drone_misbehave	✓	✗	{0, -100}	drone too low or touches the net
Penalty	drone_out_of_court	✗	✗	$[0, 0.2] \times \# \text{ step}$	\propto drone's distance out of its court
Task Reward	win_or_lose	✓	✗	{-100, 0, 100}	drone wins or loses the game
Shaping Reward	success_hit	✓	✗	$\{0, 5\} \times \# \text{ hit}$	drone hits the ball
	dist_to_ball	✗	✗	$[0, 0.5] \times \# \text{ step}$	\propto drone's distance to the ball

Table 11. Reward of multi-agent 1 vs 1 task.

Type	Name	Sparse	Shared	Value Range	Description
Misbehave	drone_misbehave	✓	✗	{0, -100}	drone too low or touches the net.
Penalty	drone_collision	✓	✗	{0, -100}	drone collides with its teammate.
Task Reward	win_or_lose	✓	✓	{-100, 0, 100}	drones win or lose the game
Shaping Reward	success_hit	✓	✓	$\{0, 10\} \times \# \text{ hit}$	drone hits the ball
	dist_to_anchor	✗	✗	$[0, 0.05] \times \# \text{ step}$	\propto drone's distance to its anchor
	dist_to_ball	✗	✗	$[0, 0.5] \times \# \text{ step}$	\propto drone's distance to the ball

Table 12. Reward of multi-agent 3 vs 3 task.

B.4. Bump and Pass

Task Definition. Drone 1 is initialized randomly around anchor 1 with position $(4.5, -2.5, 2)$, and Drone 2 is initialized randomly around anchor 2 with position $(4.5, 2.5, 2)$. The initial position of drone 1 is sampled uniformly random from $(4, -3, 1.8)$ to $(5, -2, 2.2)$, and the initial position of drone 2 is sampled uniformly random from $(4, 2, 1.8)$ to $(5, 3, 2.2)$. The ball is initialized at $(4.5, -2.5, 4)$, i.e., 2 m above anchor 1. The ball starts with zero velocity and falls freely. The drones are required to stay within a sphere with 0.5 m radius near their anchors and bump the ball to pass it to each other in turns as many times as possible. A minimum height of 4 m is required for each bump. The maximum episode length is 800 steps.

Observation and Reward. The drone's observation is a vector of dimension 39 including the drone's root state, the drone's relative position to the anchor, the drone's id, the current turn (which drone should hit the ball), the ball's relative position to the drone, the ball's velocity, and the other drone's relative position to the drone. The detailed description of the reward function of this task is listed in Table 8.

Evaluation Metric. This task is evaluated by the number of successful consecutive bumps performed by the drones. A successful bump is defined as the drone hitting the ball such that the ball's highest height exceeds 4 m and lands near the other drone.

B.5. Set and Spike (Easy)

Task Definition. Drone 1 (setter) is initialized randomly around anchor 1 with position $(2, -2.5, 2.5)$, and Drone 2 (attacker) is initialized randomly around anchor 2 with position $(2, 2.5, 3.5)$. The initial position of drone 1 is sampled uniformly random from $(1.5, -3, 2.3)$ to $(2.5, -2, 2.7)$, and the initial position of drone 2 is sampled uniformly random from $(1.5, 2, 3.3)$ to $(2.5, 3, 3.7)$. The ball is initialized at $(2, -2.5, 4.5)$, i.e., 2 m above anchor 1. The ball starts with zero velocity and falls freely. The drones are required to stay within a sphere with 0.5 m radius near their anchors. The setter is required to pass the ball to the attacker, and the attacker then spikes the ball downward to the target region in the opposing side. The target region is a circular area on the ground, centered at $(4.5, 0)$ with a radius of 1 m. The maximum episode length is 800 steps.

Observation and Reward. The drone's observation is a vector of dimension 40 including the drone's root state, the drone's relative position to the anchor, the drone's id, the current turn (how many times the ball has been hit), the ball's

relative position to the drone, the ball’s velocity, and the other drone’s relative position to the drone. The detailed description of the reward function of this task is listed in Table 9.

Evaluation Metric. This task is evaluated by the success rate of set and spike. A successful set and spike consist of four parts, (1) `setter_hit`: the setter hits the ball; (2) `attacker_hit`: the attacker hits the ball; (3) `downward_spike`: the velocity of the ball after the attacker hit is downward, i.e., $v_z < 0$; (4) `in_target`: the ball’s landing position is within the target region. The success rate is computed as $1/4 \times (\text{setter_hit} + \text{attacker_hit} + \text{downward_spike} + \text{in_target})$.

B.6. Set and Spike (Hard)

Task Definition. Drone 1 (setter) is initialized randomly around anchor 1 with position $(2, -2.5, 2.5)$, and Drone 2 (attacker) is initialized randomly around anchor 2 with position $(2, 2.5, 3.5)$. The initial position of drone 1 is sampled uniformly random from $(1.5, -3, 2.3)$ to $(2.5, -2, 2.7)$, and the initial position of drone 2 is sampled uniformly random from $(1.5, 2, 3.3)$ to $(2.5, 3, 3.7)$. The ball is initialized at $(2, -2.5, 4.5)$, i.e., $2 m$ above anchor 1. The ball starts with zero velocity and falls freely. The racket is initialized at $(-4, 0, 0.5)$, i.e., the center of the opposing side. The drones are required to stay within a sphere with $0.5 m$ radius near their anchors. The setter is required to pass the ball to the attacker, and the attacker then spikes the ball downward to the opponent’s court without being intercepted by the defense racket. The maximum episode length is 800 steps.

Observation and Reward. The drone’s observation is a vector of dimension 40 including the drone’s root state, the drone’s relative position to the anchor, the drone’s id, the current turn (how many times the ball has been hit), the ball’s relative position to the drone, the ball’s velocity, and the other drone’s relative position to the drone. The detailed description of the reward function of this task is listed in Table 10.

Evaluation Metric. This task is evaluated by the success rate of set and spike. A successful set and spike consist of four parts, (1) `setter_hit`: the setter hits the ball; (2) `attacker_hit`: the attacker hits the ball; (3) `downward_spike`: the velocity of the ball after the attacker hit is downward, i.e., $v_z < 0$; (4) `success_spike`: the ball’s landing position is within the opponent’s court without being intercepted by the defense racket. The success rate is computed as $1/4 \times (\text{setter_hit} + \text{attacker_hit} + \text{downward_spike} + \text{success_spike})$.

B.7. 1 vs 1

Task Definition. Two drones are required to play 1-vs-1 volleyball in a court of $6 m \times 3 m$. Drone 1 is initialized randomly around anchor 1 with position $(1.5, 0.0, 2.0)$, i.e., the center of the red court with height $2 m$, and Drone 2 is initialized randomly around anchor 2 with position $(-1.5, 0.0, 2.0)$, i.e., the center of the blue court with height $2 m$. The initial position of drone 1 is sampled uniformly random from $(1.4, -0.1, 1.9)$ to $(1.6, 0.1, 2.1)$, and the initial position of drone 2 is sampled uniformly random from $(-1.4, -0.1, 1.9)$ to $(-1.6, 0.1, 2.1)$. At the start of a game (i.e. an episode), one of the two drones is randomly chosen to serve the ball, which is initialized $1.5 m$ above the drone. The ball starts with zero velocity and falls freely. The game ends when one of the drones wins the game or one of the drones crashes. The maximum episode length is 800 steps.

Observation and Reward. The drone’s observation is a vector of dimension 39 including the drone’s root state, the drone’s relative position to the anchor, the drone’s id, the current turn (which drone should hit the ball), the ball’s relative position to the drone, the ball’s velocity, and the other drone’s relative position to the drone. The detailed description of the reward function of this task is listed in Table 11.

Evaluation Metric. The drone wins the game by landing the ball in the opponent’s court or causing the opponent to commit a violation. These violations include (1) crossing the net, (2) hitting the ball on the wrong turn, (3) hitting the ball with part of the drone body instead of the racket, (4) hitting the ball out of court, and (5) hitting the ball into the net.

To comprehensively evaluate the performance of strategies in the *1 vs 1* task, we consider three evaluation metrics: exploitability, win rate, and Elo rating. These metrics provide complementary insights into the quality and robustness of the learned policies.

- **Exploitability:** Exploitability is a fundamental measure of how close a strategy is to a Nash equilibrium. It is defined

as the difference between the payoff of a best response (BR) against the strategy and the payoff of the strategy itself. Mathematically, for a strategy π , the exploitability is given by:

$$\text{Exploitability}(\pi) = \max_{\pi'} U(\pi', \pi) - U(\pi, \pi),$$

where $U(\pi_1, \pi_2)$ represents the utility obtained by π_1 when playing against π_2 . The meaning of exploitability is that smaller values indicate a strategy closer to Nash equilibrium, where it becomes increasingly difficult to exploit. Since exact computation of exploitability is often infeasible in real-world tasks, we instead use approximate exploitability. In this task, we fix the strategy on one side and train an approximate best response on the other side to maximize its utility, i.e., win rate. The difference between the BR's win rate and the evaluated policy's win rate then serves as the approximate exploitability.

- **Win Rate:** Since exact exploitability is challenging to compute, a practical alternative is to evaluate the win rate through cross-play with other learned policy populations. Specifically, we compute the average win rate of the evaluated policy when matched against other learned policies. Higher average win rates typically suggest stronger strategies. However, due to the transitive nature of zero-sum games (Czarnecki et al., 2020), a high win rate against specific opponent populations does not necessarily imply overall mastery of the game. Thus, while win rate is a useful reference metric, it cannot be the sole criterion for assessing strategy strength.
- **Elo Rating:** Elo rating is a widely used metric for evaluating the relative strength of strategies within a population. It is computed based on head-to-head match results, where the expected win probability between two strategies is determined by their Elo difference. After each match, the Elo ratings of the strategies are updated based on the match outcome. While a higher Elo rating indicates better performance within the given population, it does not necessarily imply proximity to Nash equilibrium. A strategy with a higher Elo might simply be more effective against the specific population, rather than being universally robust. Therefore, Elo complements exploitability by capturing population-specific relative performance.

B.8. 3 vs 3

Task Definition. The task involves two teams of drones competing in a 3-vs-3 volleyball match within a court of $9\text{ m} \times 4.5\text{ m}$. Drone 1, Drone 2, and Drone 3 belong to *Team 1* and are initialized at positions $(3.0, -1.5, 2.0)$, $(3.0, 1.5, 2.0)$ and $(6.0, 0.0, 2.0)$ respectively. Similarly, Drone 4, Drone 5, and Drone 6 belong to *Team 2* and are initialized at positions $(-3.0, -1.5, 2.0)$, $(-3.0, 1.5, 2.0)$ and $(-6.0, 0.0, 2.0)$ respectively. At the start of a game (i.e., an episode), one of the two teams is randomly selected to serve the ball. The ball is initialized at a position 3 m directly above the serving drone. The ball starts with zero velocity and falls freely. The game ends when one of the teams wins the game or one of the drones crashes. The maximum episode length is 500 steps.

Observation and Reward. The drone's observation is a vector of dimension 57 including the drone's root state, the drone's relative position to the anchor, the ball's relative position to the drone, the ball's velocity, the current turn (which team should hit the ball), the drone's id, a flag indicating whether the drone is allowed to hit the ball, and the other drone's positions. The detailed description of the reward function of this task is listed in Table 12.

Evaluation Metric. Similar to the *1 vs 1* task, either of the two teams wins the game by landing the ball in the opponent's court or causing the opponent to commit a violation. These violations include (1) crossing the net, (2) hitting the ball on the wrong turn, (3) hitting the ball with part of the drone body, rather than the racket, (4) hitting the ball out of court, and (5) hitting the ball into the net. The task performance is also evaluated by the three metric metrics including exploitability, win rate, and Elo as described in the *1 vs 1* task.

C. Discussion of Benchmark Algorithms

C.1. Reinforcement Learning Algorithms

To explore the capabilities of our testbed while also providing baseline results, we implement and benchmark a spectrum of popular RL and game-theoretic algorithms on the proposed tasks.

hyperparameters	value	hyperparameters	value	hyperparameters	value
critic lr	5×10^{-4}	actor lr	5×10^{-4}	share actor	true
optimizer	Adam	actor and critic network	MLP	MLP hidden sizes	[256, 128, 128]
max grad norm	10	buffer length	64	buffer size	6×10^6
batch size	16384	gamma	0.95	exploration noise	0.1
tau	0.005	target update interval	4	critic loss	smooth L1
max episode length	800	num envs	4096	train steps	1×10^9

Table 13. Hyperparameters used for (MA)DDPG in single-agent tasks and multi-agent tasks.

Single-Agent RL. In single-agent scenarios, we consider two commonly used algorithms in continuous control tasks. Deep Deterministic Policy Gradient (DDPG) (Lillicrap, 2015) is an off-policy actor-critic approach relying on a deterministic policy and an experience replay buffer to handle continuous actions. Proximal Policy Optimization (PPO) (Schulman et al., 2017) adopts a clipped objective to stabilize on-policy learning updates by constraining policy changes. Overall, these methods provide contrasting paradigms for tackling single-agent continuous tasks.

Multi-Agent RL. For tasks with multiple drones, we evaluate four representative multi-agent algorithms. Multi-Agent DDPG (MADDPG) (Lowe et al., 2017) extends DDPG with a centralized critic for each agent, while policies remain decentralized. Multi-Agent PPO (MAPPO) (Yu et al., 2022) incorporates a shared value function to improve both coordination and sample efficiency. Heterogeneous-Agent PPO (HAPPO) (Kuba et al., 2021) adapts PPO techniques to handle distinct roles or capabilities among agents. Multi-Agent Transformer (MAT) (Wen et al., 2022) leverages a transformer-based architecture to enable attention-driven collaboration. Taken together, these algorithms offer a diverse set of baselines for multi-agent cooperation.

Game-Theoretic Algorithms. For multi-agent competitive tasks, we consider several representative game-theoretic algorithms in the literature (Zhang et al., 2024). Self-play (SP) trains agents against the current version of themselves, allowing a single policy to evolve efficiently. Fictitious Self-Play (FSP) (Heinrich et al., 2015) trains agents against the average policy by maintaining a pool of past checkpoints. Policy-Space Response Oracles (PSRO) (Lanctot et al., 2017) iteratively add the best responses to the mixture of a growing policy population. The mixture policy is determined by a meta-solver. PSRO_{uniform} uses a uniform meta-solver that samples policies with equal probability, while PSRO_{Nash} uses a Nash meta-solver that samples policies according to the Nash equilibrium. These methods provide an extensive benchmark for game-theoretic algorithms in multi-agent competition with both motion control and strategic play. There are also some algorithms like Team-PSRO (McAlear et al., 2023) and Fictitious Cross-Play (FCP) (Xu et al., 2023) that are designed specifically for mixed cooperative-competitive games and can be integrated in our testbed in future work.

D. Details of Benchmark Experiments

D.1. Hyperparameters of Benchmarking Algorithms

D.1.1. SINGLE-AGENT TASKS.

The hyperparameters adopted for DDPG and PPO in the single-agent tasks are listed in Table 13-15. All algorithms are trained for 5×10^8 environment steps in each task.

D.1.2. MULTI-AGENT COOPERATIVE TASKS

The hyperparameters adopted for different algorithms in multi-agent cooperative tasks are listed in Table 13-15. All algorithms are trained for 1×10^9 environment steps in each task.

D.1.3. MULTI-AGENT COMPETITIVE TASKS.

Training. For self-play (SP) in *1 vs 1* and *3 vs 3* competitive tasks, we adopt the MAPPO algorithm with shared actor networks and shared critic networks between two teams, in order to make sure two teams utilize the same policy. Also, we transform the samples from both sides into symmetric ones and then use these symmetric samples to update the

hyperparameters	value	hyperparameters	value	hyperparameters	value
optimizer	Adam	max grad norm	10	entropy coef	0.001
buffer length	64	num minibatches	16	ppo epochs	4
value norm	ValueNorm1	clip param	0.1	normalize advantages	True
use huber loss	True	huber delta	10	gae lambda	0.95
use orthogonal	True	gain	0.01	gae gamma	0.995
max episode length	800	num envs	4096	train steps	1×10^9

Table 14. Common hyperparameters used for (MA)PPO, HAPPO, and MAT in single-agent tasks and the multi-agent tasks.

Algorithms	(MA)PPO	HAPPO	MAT
actor lr	5×10^{-4}	5×10^{-4}	3×10^{-5}
critic lr	5×10^{-4}	5×10^{-4}	3×10^{-5}
share actor	True	False	/
hidden sizes	[256, 128, 128]	[256, 128]	[256, 256, 256]
num blocks	/	/	3
num head	/	/	8

Table 15. Different hyperparameters used for (MA)PPO, HAPPO, and MAT in the single-agent tasks and multi-agent tasks.

network together. The hyperparameters employed here are the same as those used in the MAPPO algorithm for multi-agent cooperative tasks.

The PSRO algorithm for *1 vs 1* competitive task instantiates a PPO agent for training one of the two drones while the other drone maintains a fixed policy. Similarly, the PSRO algorithm for the *3 vs 3* task assigns each team to be controlled by MAPPO. We adopt the same set of hyperparameters listed in Table 15 for the (MA)PPO agent. In each iteration, the (MA)PPO agent is trained against the current population. Here, we offer two versions of meta-strategy solver, PSRO_{Uniform} and PSRO_{Nash}. Training is considered converged when the agent achieves over 90% win rate with a standard deviation below 0.05. The iteration ends when the agent reaches convergence or reaches a maximum of iteration steps of 5000. The trained actor is then added to the population for the next iteration.

For Fictitious Self-Play (FSP) in competitive tasks, we slightly modify PSRO_{Uniform} so that in each iteration, the (MA)PPO agent inherits the learned policy from the previous iteration as initialization. Naturally, other hyperparameters and settings remain the same for a fair comparison.

In both *1 vs 1* and *3 vs 3* tasks, the algorithm leverages 2048 parallel environments to accelerate the training process. In this work, we report the results of different algorithms given a total budget of 1×10^9 environmental steps.

Evaluation. The evaluation of exploitability requires evaluating the payoff of the best response (BR) over the trained policy or population from different algorithms. Here, we approximate the BR to each policy or population by learning an additional RL agent against the trained policy or population. In practice, this is done by performing an additional iteration of PSRO, where the opponent is fixed as the trained policy/population. In order to approximate the ideal BR as closely as possible, we initialize the BR policy with the latest FSP policy, given that FSP yields the best empirical performance in our experiments. We train the BR policy for 5000 training step with 2048 parallel environments. We disable the convergence condition for early termination and report the evaluated win rate to calculate the approximate exploitability. Importantly, to approximate the BR of the trained SP policy in the *3 vs 3* task, we employ two distinct BR policies for the serve and rally scenarios, respectively. For the BR to serve, we directly use the latest FSP policy without further training, while for the BR to rally, we train a dedicated policy against the SP policy. The overall win rate of this BR is then computed as the average win rate across these two scenarios, given that each side has an equal serve probability of 0.5.

We run 1,000 games for each pair of policies to generate the cross-play win rate heatmap, covering 6 matchup scenarios, resulting in a total of 6,000 games. In each game, both policies are sampled from their respective policy populations based on the meta-strategy and play until a winner is determined.

Moreover, we use an open-source Elo implementation (Sheehan, 2017). The coefficient K is set to 168, and the initial Elo

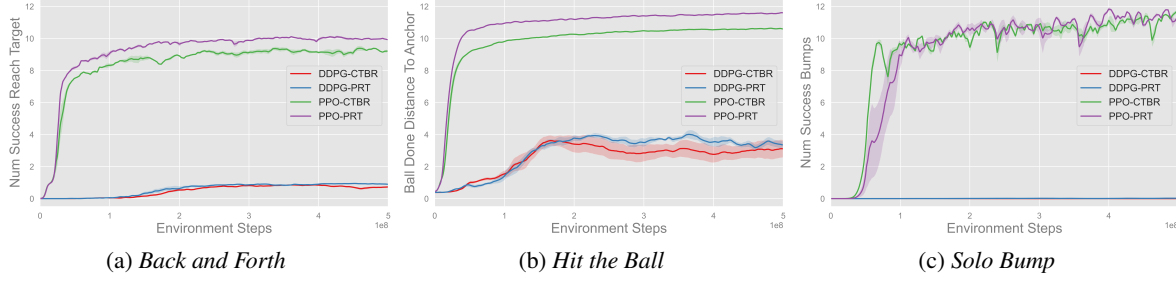


Figure 6. Training curves of single-agent tasks over three seeds.

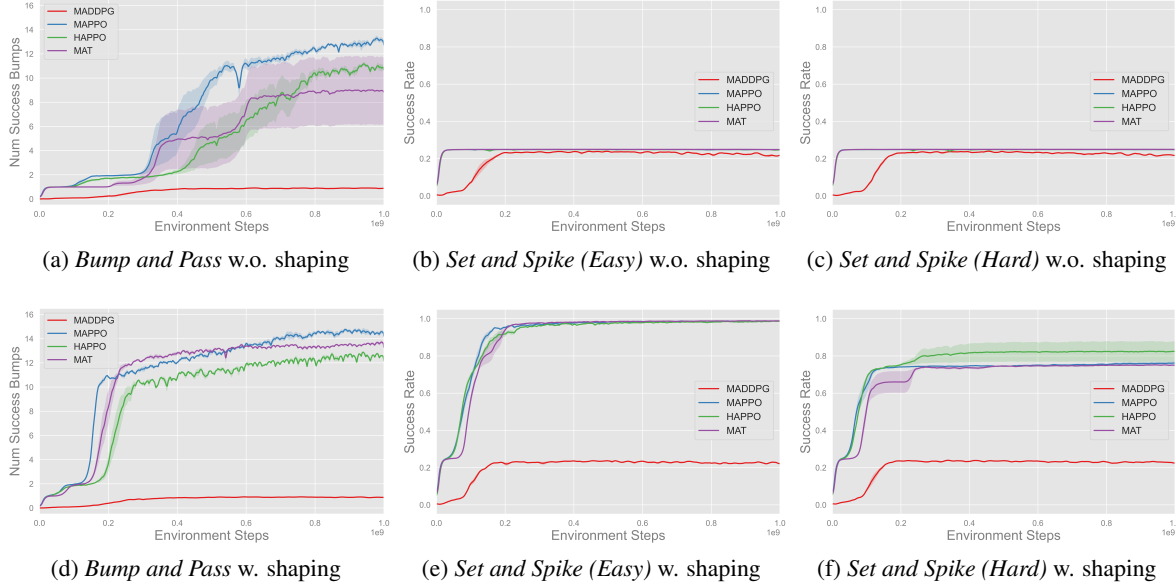


Figure 7. Training curves of multi-agent cooperative tasks over three seeds.

rating for all policies is 1000. We conduct 12000 games among four policies. The number of games played between any two policies is guaranteed to be the same. Specifically, in each round, 6 different matchups are played. Each policy participates in 3 matchups, competing against different opponent policies. A total of 2000 rounds are carried out, amounting to 12000 games in total. The game results are sampled and generated based on the cross-play results.

D.2. Results of Single-Agent Tasks

The training curves of DDPG and PPO in single-agent tasks are shown in Fig. 6. It can be seen that PPO outperforms DDPG in all tasks. For example, in Back and Forth, using PPO, the number of times the agent reaches the target anchor stabilizes around 9 – 10, and the task is successfully completed. In contrast, with DDPG, the agent only completes half of the return motion, as the drone ends up flying out of bounds. In Hit the Ball, with PPO, the hitting distance stabilizes around 10 – 11 m, and the ball is almost always hit in a straight line. However, with DDPG, the landing spot of the ball is less controllable. In Solo Bump, with PPO, the ball juggles smoothly, reaching a height of 4 m, while DDPG almost fails to juggle properly and can only manage a single hit. CTBR and PRT are comparable. in Back and Forth and Hit the Ball PRT's final result is better, in Solo Bump is comparable but CTBR learns faster.

D.3. Results of Multi-Agent Cooperative Tasks

The training curves of different algorithms in multi-agent tasks are shown in Fig. 7. It can be seen that MAPPO, HAPPO, and MAT are able to complete the tasks relatively well, while MADDPG can only make the setter complete one hit, with

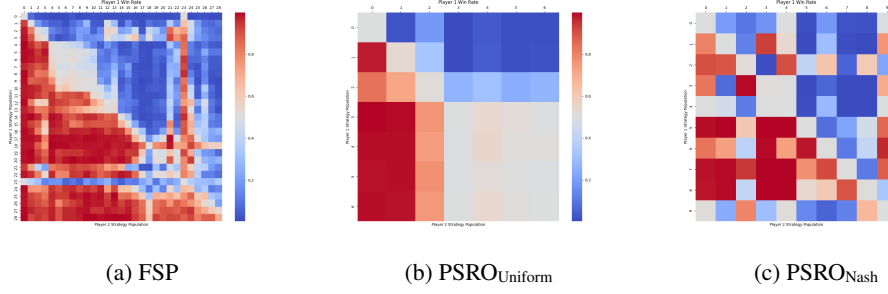


Figure 8. Win rate heatmaps of the population in the *1 vs 1* task.

the attacker unable to receive the ball. In Bump and Pass w.o. shaping, MAPPO maintains a fast training process and outperforms HAPPO and MAT in terms of final results. The same is true in Set and Spike (Easy and Hard) w.o. shaping. In Set and Spike (Easy) w. shaping, MAPPO, and HAPPO perform similarly, with slightly faster learning speeds than MAT. In Set and Spike (Hard) w. shaping task, HAPPO only succeeds in overcoming the defense racket in one seed, resulting in a success rate of approximately 0.82. At this point, the ball can be quickly spiked into the opponent’s court and the attacker doesn’t touch the net. Overall, the success rate is slightly higher than MAPPO and MAT, as these two algorithms almost never successfully overcome the defense racket.

Additionally, we can observe that the presence of shaping rewards has a significant impact on task results. Adding shaping rewards clearly improves the performance and accelerates the learning process. In Bump and Pass, the task learns slower without shaping rewards because the policy must explore which direction to hit the ball, requiring many more steps. The hit direction reward in shaping rewards accelerates this process. In Set and Spike (Easy), all algorithms without shaping rewards have a success rate of only 0.25 because they only learn to make the setter hit the ball, but not toward the hitter. As a result, the attacker fails to hit the ball. The hit direction reward in shaping rewards also helps accelerate this process. In Set and Spike (Hard), HAPPO achieves a success rate of about 0.82, while MAPPO and MAT are slightly worse, at 0.75, because the defense racket is strong and successfully intercepts their attacks.

D.4. Results of Multi-Agent Competitive Tasks

We provide a more detailed win rate evaluation of the PSRO populations from the *1 vs 1* task in Fig. 8, where each policy in the PSRO population is evaluated against all other policies. In these heatmaps, the ordinate and abscissa represent the policy for drone 1 and drone 2 respectively. The heat of cells represents the evaluated win rate of drone 1, i.e. red means a higher win rate and blue means a lower win rate. Intuitively, each row represents a policy’s performance against each policy of the population while playing as drone 1. A red cell indicates that the drone 1 policy outperforms the specific drone 2 policy. A full red row means that the policy outperforms all other policies.

Evidently, FSP attains more iterations than PSRO_{Uniform} and PSRO_{Nash} given a budget of 1×10^9 steps, which yields a faster convergence speed. This advantage comes from the fact that FSP inherits the learned policy from the previous iteration, which serves as an advantageous initialization for the current iteration. In contrast, PSRO_{Uniform} and PSRO_{Nash} start from scratch in each iteration, which poses a challenge for the algorithm to converge and introduces more variance in the training process.

Moreover, in PSRO algorithms, as the learned policy gradually improves with each iteration, the most recent policy of the population naturally poses greater difficulty for subsequent iterations. Therefore, PSRO_{Nash} tends to put more weight on the most recent policy in the meta-strategy. This in turn has an effect on the learning of new policies. We can observe the outcomes in the heatmaps: for each row, the win rate against the most recent policy is often higher than the others. In FSP, on the other hand, the win rate against each policy is more evenly distributed, indicating that the population is potentially more balanced and stable.

D.5. Low-level Skills of Hierarchical Policy

Low-level skills are derived through PPO training, while the high-level skill is implemented as a rule-based, event-driven policy that determines which drone utilizes which skill in response to the current game state. In accordance with the *3 vs 3* task setting, each team consists of three drones positioned as front-left, front-right, and backward within their half of the court. Below, we describe each low-level skill and explain when it is utilized by the high-level policy.

Hover. The *Hover* skill is designed to enable the drone to hover around a specified target position. This skill takes a three-dimensional target position as input. The skill is frequently utilized by the high-level policy. For instance, in the serve scenario, only the serving drone uses the *Serve* skill, while the other two teammates use the *Hover* skill to remain at their respective anchor points.

Serve. The *Serve* skill is designed to enable the drone to serve the ball towards the opponent’s side of the court. This skill includes a one-hot target input that determines whether to serve the ball to the left side or the right side of the opponent’s court. In accordance with the *3 vs 3* task setting, for the *Serve* skill, the ball is initialized at a position 3 m directly above the serving drone, with zero initial velocity. This skill is exclusively utilized by the high-level policy during the serve scenario, during which the designated serving drone employs the *Serve* skill at the start of a match.

Pass. The *Pass* skill is designed to handle the opponent’s serve or attack by allowing the drone to make the first contact of the team’s turn and pass the ball to a teammate. Here, this skill is exclusively used by the backward drone, which is responsible for hitting the ball to the front-left teammate. The high-level policy designates the backward drone to utilize this skill whenever the opponent hits the ball.

Set. The *Set* skill is designed to transfer the ball from the passing drone to the attacking drone, serving as the second contact in the team’s turn. In our design, the front-left drone utilizes the *Set* skill to pass the ball from the backward drone to the front-right drone. The high-level policy designates the front-left drone to utilize this skill whenever the backward drone successfully makes contact with the ball.

Attack. The *Attack* skill is designed to hit the ball towards the opponent’s court, serving as the third and final contact in the team’s turn. This skill includes a one-hot target input that specifies whether to direct the ball to the left side or the right side of the opponent’s court. In our design, the front-right drone uses the *Attack* skill to strike the ball after receiving it from the front-left drone. The high-level policy assigns the front-right drone to utilize this skill whenever the front-left drone successfully hits the ball.

D.6. Sim-to-Real

The sim-to-real gap presents a significant challenge in RL-based robotic control, as policies trained in simulation often underperform when deployed in the real world. We utilize the *Solo Bump* task as an initial demonstration to showcase the potential of transferring trained policies to real-world scenarios. To bridge the sim-to-real gap, we apply system identification to accurately model the ball’s behavior during its impact with the racket.

The impact between the ball and the racket is modeled as an impulse acting in the direction of the normal of the racket \mathbf{n}_c , which means that the tangential velocity of the ball relative to the racket remains constant but the normal velocity changes, determined by the restitution coefficient. Since the mass of the racket and vehicle (rigidly mounted together) is much larger than that of the ball, it is assumed that the velocity of the racket remains unaffected. Denoting the ball’s pre- and post-impact normal velocities relative to the racket as $\mathbf{v}_{ball_pre_n}$ and $\mathbf{v}_{ball_post_n}$, the restitution coefficient can be derived as follows:

$$\beta = -\frac{\mathbf{v}_{ball_post_n}^T \mathbf{n}_c}{\mathbf{v}_{ball_pre_n}^T \mathbf{n}_c} \quad (9)$$

Specifically, the restitution coefficient was measured through multiple experiments in which the racket and vehicle were fixed on the flat ground and the ball started a free fall from different heights right above the center of the racket. The pre-impact and post-impact velocity of the ball was collected using a motion capture system and the restitution coefficient was calculated using the above equation. We used the same ball and racket in all experiments.

The average restitution coefficient was 0.8, which we used in the simulation. The highest and lowest were 0.85 and 0.75, respectively, and the deviation was relatively small and acceptable. Experiments also showed that the ball's tangential velocity did change during impact, which was likely due to the friction between the ball and the racket. In addition, the asymmetric relative position from racket strings to the ball could lead to asymmetric force upon the ball, causing it to move tangentially. We model the change of tangential velocity of the ball during impact as a stochastic process and utilize small randomization in the ball's rebound velocity after each collision in the simulation.